Acta Biomaterialia 11 (2015) 449–458

Contents lists available at ScienceDirect

Acta Biomaterialia

journal homepage: www.elsevier.com/locate/actabiomat

Engineering a vascularized collagen-β-tricalcium phosphate graft using an electrochemical approach

Yunqing Kang [a], Naoto Mochizuki [b], Ali Khademhosseini [c,d,e], Junji Fukuda [f,b,*], Yunzhi Yang [a,g,*]

[a] Department of Orthopedic Surgery, Stanford University, 300 Pasteur Drive, Stanford, CA 94305, USA
[b] Graduate School of Pure and Applied Sciences, University of Tsukuba, 1-1-1 Tennodai, Tsukuba, Ibaraki 305-8573, Japan
[c] Biomaterials Innovation Research Center, Division of Biomedical Engineering, Department of Medicine, Brigham and Women's Hospital, Harvard Medical School, Cambridge, MA 02139, USA
[d] Harvard-MIT Division of Health Sciences and Technology, Massachusetts Institute of Technology, Cambridge, MA 02139, USA
[e] Wyss Institute for Biologically Inspired Engineering, Harvard University, Cambridge, MA 02139, USA
[f] Graduate School of Engineering, Yokohama National University, 79-5 Tokiwadai, Hodogaya-ku, Yokohama 240-8501 Japan
[g] Department of Materials Science and Engineering, Stanford University, 300 Pasteur Drive, Stanford, CA 94305, USA

ARTICLE INFO

Article history:
Received 4 April 2014
Received in revised form 16 September 2014
Accepted 21 September 2014
Available online 28 September 2014

Keywords:
Electrochemical
Microchannel
Vascularization
Collagen
β-Tricalcium phosphate

ABSTRACT

Vascularization of three-dimensional large synthetic grafts for tissue regeneration remains a significant challenge. Here we demonstrate an electrochemical approach, named the cell electrochemical detachment (CED) technique, to form an integral endothelium and use it to prevascularize a collagen-β-tricalcium phosphate (β-TCP) graft. The CED technique electrochemically detached an integral endothelium from a gold-coated glass rod to a collagen-infiltrated, channeled, macroporous β-TCP scaffold, forming an endothelium-lined microchannel containing graft upon removal of the rod. The in vitro results from static and perfusion culture showed that the endothelium robustly emanated microvascular sprouting and prevascularized the entire collagen/β-TCP integrated graft. The in vivo subcutaneous implantation studies showed that the prevascularized collagen/β-TCP grafts established blood flow originating from the endothelium-lined microchannel within a week, and the blood flow covered more areas in the graft over time. In addition, many blood vessels invaded the prevascularized collagen/β-TCP graft and the in vitro preformed microvascular networks anastomosed with the host vasculature, while collagen alone without the support of rigid ceramic scaffold showed less blood vessel invasion and anastomosis. These results suggest a promising strategy for effectively vascularizing large tissue-engineered grafts by integrating multiple hydrogel-based CED-engineered endothelium-lined microchannels into a rigid channeled macroporous scaffold.

1. Introduction

Synthetic calcium phosphate (CaP) bioceramics have been extensively used in bone repair as alternatives to autografts and allografts due to their excellent biocompatibility and osteoconductivity [1–3]. However, using CaP scaffolds to repair large bone defects caused by traumas, tumors or fractures remains a challenge mainly due to insufficient vascularization. Therefore, it is crucial to improve the vascularization of large bone grafts for tissue survival and engraftment [4–6]. Current strategies of prevascularizing CaP scaffolds mainly include applying angiogenic growth factors [7–10], monoculturing endothelial cells or co-culturing endothelial and bone progenitor cells [11,12] on the scaffolds or inserting a vascular bundle in the scaffolds [13,14]. However, these strategies demonstrate limited abilities in prevascularizing grafts or need extra surgical procedures to assemble the bundle [8,10,15,16].

Instead of these methods, creating vessel-like microchannels in a hydrogel-based matrix has been proposed to promote prevascularization, under the assumption that vessel-like microchannels can improve the nutrition and oxygen supply to the large graft and facilitate vascularization [17–19]. Currently, many approaches such as layer-by-layer assembly [20–23], three-dimensional (3-D) sacrificial molding [24–26], bioprinting [27] and photolithography [28,29] have been developed to fabricate microchannels. These approaches are generally based on a hydrogel matrix and typically create a hollow channel in the hydrogel first, followed by perfusing an endothelial cell suspension into the channel. Endothelial cells then attach to the inner surface of the channel and reorganize

* Corresponding authors at: Graduate School of Pure and Applied Sciences, University of Tsukuba, 1-1-1 Tennodai, Tsukuba, Ibaraki 305-8573, Japan (J. Fukuda). Department of Orthopedic Surgery, Stanford University, 300 Pasteur Drive, Stanford, CA 94305, USA (Y. Yang).
E-mail addresses: fukuda@ynu.ac.jp (J. Fukuda), ypyang@stanford.edu (Y. Yang).

http://dx.doi.org/10.1016/j.actbio.2014.09.035
1742-7061/

themselves to form an endothelium [20,22,30,31]. One challenge of these strategies is to effectively integrate such hydrogel-based microchannels into a rigid porous scaffold [23,25,26].

Recently, a cell electrochemical detachment (CED) technique has been developed to engineer an intact endothelium in collagen hydrogel [32,33]. This process involves culturing human umbilical vein endothelial cells (HUVECs) onto an oligopeptide-coated glass rod to confluence, casting a collagen hydrogel around the glass rod in a customized chamber and subsequently detaching the cells to the casted collagen gel through the electrochemical detachment technique, thus resulting in an integral endothelium-lined microchannel upon removal of the rod [32,31,33]. The principle behind this CED technique is that the cell-adhesive RGD-containing oligopeptide is sensitive to electric potentials [31,33,34]. When an electrical potential is applied, the chemical bond between the oligopeptide and the gold-coated glass surface is cleaved, and an intact endothelium layer is detached and adhered onto the surrounding hydrogel (Fig. 1a and Fig. S.1).

In this study we propose to use this electrochemical approach, CED, to engineer an endothelium and use it to prevascularize a collagen-β-tricalcium phosphate (β-TCP) graft. More specifically, we utilized this CED technique to fabricate an endothelium-lined microchannel in a collagen infiltrated, channeled, macroporous β-TCP scaffold to facilitate prevascularization. Our hypothesis is that the CED-engineered endothelium-lined microchannel can promote rapid prevascularization of the entire graft in vitro and establish blood flow in vivo. To test the hypothesis we fabricated an endothelialized microchannel in a collagen hydrogel (Collagen/HUVEC) and in a collagen infiltrated, channeled, macroporous β-TCP scaffold (Collagen/HUVEC/β-TCP). As controls, we used the same plain glass rods without HUVECs to make a microchannel in a collagen hydrogel (Collagen/Channel) and in a collagen infiltrated, channeled, macroporous β-TCP scaffold (Collagen/Channel/β-TCP). We studied in vitro cell migration and microvascular network formation in the graft under static culture and perfusion conditions. Furthermore, we subcutaneously implanted the in vitro prevascularized grafts into nude mice to investigate their angiogenic and anastomotic ability in vivo.

2. Materials and methods

2.1. Materials and reagents

Collagen type I (Cell matrix Type I-A; 3 mg ml^{-1} in Dulbecco's phosphate-buffered saline (DPBS); pH = 7.4, Nitta Gelatin) was

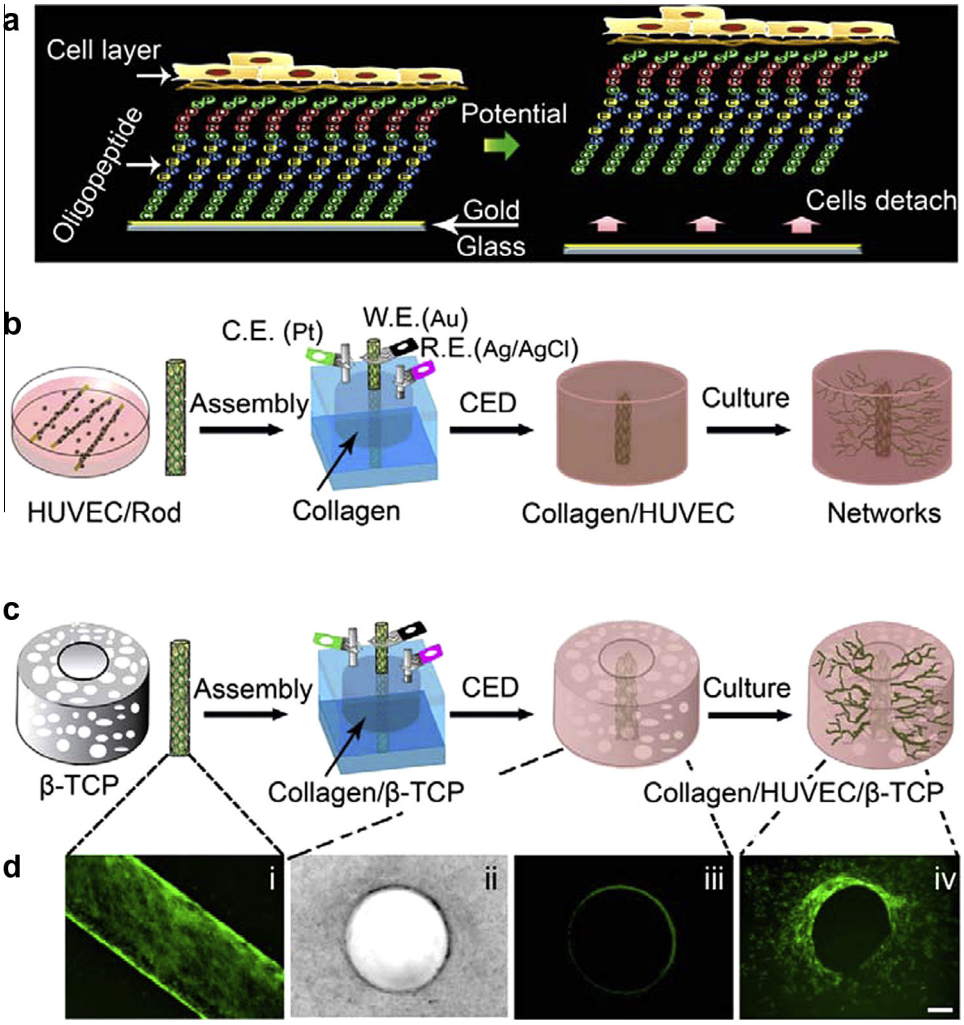

Fig. 1. Fabrication of a microchannel in hydrogel-based or hydrogel-ceramic-based constructs. (a) A schematic shows the mechanism of the cell electrochemical detachment (CED) technique. (b, c) Schematic diagrams show the assembly procedures of a microchannel in a type I collagen hydrogel and in a collagen-β-TCP graft using the CED technique. (d) (i) a fluorescent image of HUVECs on an oligopeptide-coated rod, (ii) a bright-field image of a microchannel in collagen (top view), (iii) a fluorescent image of a microchannel in collagen (top view) and (iv) a fluorescent image of networks sprouting from the microchannel into the surrounding area of the graft (top view) (scale bar = 100 μm).

purchased from Wako Chemicals USA, Inc. (Richmond, VA). β-TCP powder with a specific surface area of 17 $m^2 g^{-1}$ was obtained from Nanocerox, Inc. (Ann Arbor, Michigan). Paraffin granules were purchased from Fisher Scientific (Pittsburgh, USA). EBM™ (endothelial basal medium) and EGM™ (endothelial growth media) Single Quots™ Kits were purchased from Lonza, Inc. Anti-human CD31 (PECAM-1) primary antibody was obtained from Cell Signaling (89C2, Billerica, MA), and the secondary antibody Alexa Fluor® 594 (goat anti-mouse, 2 mg ml^{-1}) was purchased from Invitrogen (Carlsbad, CA).

2.2. Preparation of porous β-TCP scaffolds

Porous β-TCP scaffolds with a central channel were prepared by a template-casting method described in previous studies [35,36]. Briefly, β-TCP powder with 60 mesh purchased from Nanocerox Inc. (Ann Arbor, MI), dispersant (Darvan® C), surfactant (Surfonal®) and carboxymethyl cellulose powder were mixed in distilled water to form β-TCP ceramic slurry. The slurry was then cast into a customized mold packed with paraffin beads of 710–1000 μm diameter. Following casting, graded dehydration, demolding and sintering were performed. The prepared scaffolds were ~8 mm in diameter and 5 mm in height. The central channel in the scaffold was 3 mm in diameter. The pore size of the β-TCP scaffold is ~350–500 μm [35,37].

2.3. Cell culture

Green fluorescent protein-expressing HUVECs were provided from the laboratory of the late Dr J. Folkman (Children's Hospital, Boston). The HUVECs were cultured in EBM-2, which contains supplements from the EGM-2 kit, 10% fetal bovine serum (FBS) and 1× penicillin-streptomycin-glutamine (PSG, Invitrogen). The cell medium was changed every 3 days. Cells below passage 9 were used in all the experiments.

2.4. Growth of HUVECs on glass rods

The procedure of seeding HUVECs on oligopeptide coated glass rods has been described previously [32–34]. First, a glass rod of 600 μm in diameter was sputter-coated with a thin layer of chromium followed by gold. Then, the gold-coated rods were sterilized with 70% ethanol for three times and 15 min each time. After extensive washing with phosphate buffered saline (PBS), the rods were immersed in 1 μM RGD-containing oligopeptide solution overnight at 4 °C and washed with distilled water. The sequence of the oligopeptide was CGGGKEKEKEKGRGDSP, consisting of an RGD domain inside for cell attachment and cysteine residues at the end for bonding to the gold surface. The electrostatic force between the neighboring molecules of the alternate K (lysine) and E (glutamic acid) sequence leads to the formation of a closely packed self-assembled monolayer. Three oligopeptide-absorbed gold-coated glass rods were placed into a 35 mm non-adherent culture dish (Thermo Scientific Nunc Hydrocell). 2 ml HUVEC suspension containing 3×10^5 cells was added into the dish. HUVECs grew and reached confluence on the rods within 5–7 days.

2.5. Fabrication of a collagen microchannel in the scaffold

Fig. 1 shows a schematic using CED for fabricating a collagen microchannel and its integration with a channeled ceramic scaffold. To apply the CED technique, a customized chamber was designed to facilitate cell transfer to the collagen-based or collagen-β-TCP-based scaffolds. All the assembling parts for a chamber were sterilized in 70% ethanol three times and for 15 min each time followed by extensive washing in PBS. The sterile collagen solution was prepared in a biological safety cabinet according to the manufacturer's instruction. After confirming that HUVECs were confluent on rods using fluorescent microscopy, a rod with HUVECs was gently inserted into the central hole of the chamber (Fig. S.1), followed by casting the prepared collagen solution into the chamber (Fig. 1b). To make a collagen microchannel in the β-TCP scaffold, the channeled porous β-TCP scaffold, which was sterilized in an autoclave, was put in the chamber first, followed by inserting the cell-covered rod and casting the prepared collagen solution (Fig. 1c). After collagen gelled for 30 min at 37 °C, a potential of −1.0 V for 5 min was applied to the rods with respect to an Ag/AgCl reference electrode to detach the cells from the rod onto the collagen matrix. The rod was then gently removed and a microchannel with a diameter of 600 μm was formed. The samples were removed from the chamber and incubated in static culture for 1, 3 and 7 days. To investigate the effect of perfused medium on the network formation of endothelial cells in the microchannel, three samples in the chambers were not removed. The assembled chambers were directly incubated in static medium overnight to allow cell attachment and then connected to a syringe pump using a 10 μl pipette tip which was inserted into the microchannel and linked to a tube. The culture medium was pumped to go through the microchannel at a rate of 10 μl min^{-1} for 7 days (see Supplementary materials). Four groups of samples were used in our experiments: Group 1 was the collagen with a microchannel but without HUVECs in the inner surface of the microchannel, labeled as Collagen/Channel; Group 2 was the collagen with an endothelialized microchannel, as Collagen/HUVEC; Group 3 was the collagen infiltrated, single-channeled macroporous β-TCP scaffold with a non-endothelialized microchannel, as Collagen/Channel/β-TCP; and Group 4 was the collagen infiltrated, single-channeled macroporous β-TCP scaffold with the endothelialized microchannel, as Collagen/HUVEC/β-TCP.

2.6. In vitro network formation

To observe the morphology of HUVECs on the microchannel of Collagen/HUVEC and Collagen/HUVEC/β-TCP, the samples in the static culture were removed from the chamber and fixed for observation by a fluorescent microscope. To visualize the formation of capillary-like networks in Collagen/HUVEC or Collagen/HUVEC/β-TCP, immunofluorescent staining for human CD31 was performed. At designated time points, the specimens were fixed in 4% paraformaldehyde and then blocked in 5% goat serum blocking buffer for 1 h. Primary antibody mouse anti-human CD31 (89C2, cell signaling technology, dilution 1:3200) in 1% bovine serum albumin (BSA)-PBS was added to the sample followed by incubation overnight at 4 °C. Secondary antibody goat-anti-mouse (Alexa Fluor® 594, 2 μg ml^{-1}, Invitrogen) in 1% BSA-PBS was added to the samples and incubated in the dark for 1 h at room temperature. Finally, the cell nuclei were counterstained with DAPI (5 μg ml^{-1}) for 1 min and then extensively washed with PBS. A confocal microscope was used to capture the fluorescent staining images (Zeiss LSM 510). To observe the formation of branching networks from the cross-section of the microchannel, a Collagen/HUVEC sample was embedded in paraffin and sectioned. Immunofluorescent staining was also performed on the 7 μm paraffin sections.

2.7. In vivo implantation

Angiogenesis and anastomosis of the engineered collagen/β-TCP grafts in vivo were evaluated by implanting the grafts into immunodeficient mice. In this study male immunodeficient nude mice (6 to 7 week olds, 20–25 g body weight, Charles River Laboratories, Wilmington, MA) were used to implant the grafts. Before the surgeries, the grafts of four groups, including Collagen/Channel,

Collagen/HUVEC, Collagen/Channel/β-TCP and Collagen/HUVEC/β-TCP, were prepared and cultured in static EBM-2 medium for 7 days. The grafts of the four groups were surgically implanted into subcutaneous pockets on the backs of the nude mice. One graft from each of the four groups was implanted per mouse. Eight mice were used for each experimental condition. After the surgeries, 25 μg cefazolin/g and 0.1 μg buprenorphine/g per g body weight were administered, and each mouse was individually housed. After 7 and 14 days, eight mice were sacrificed for histological analysis. All animal studies were reviewed and approved by the Administrative Panel on Laboratory Animal Care (APLAC) of Stanford University.

2.8. In vivo imaging of vascular volume and blood flow on live mice

At each time point, four mice received vasculature volume assessment using a photoacoustic (PA) imaging system (Visual Sonics Vevo LZAR system). After each mouse was fixed on a precision xyz-stage, an ultrasound hydrogel was applied to the skin, and a focused transducer probe with a frequency of 21 MHz frequency was used to acquire bright-field and photoacoustic images at a wavelength of 720 nm. Two-dimensional real-time B-mode scanning was first used to visualize the location of the scaffold. Then B-mode was switched to PA mode. The PA image was overlaid on the B-mode image to identify the location of new blood vessels in the samples. To study whether the blood flowed throughout, an implanted scaffolds, a high-frequency Doppler power system (Visual Sonics Vevo 2100) was used to detect the signal of blood flow. The ultrasound transducer with a frequency of 33 MHz was positioned above the location of the scaffold beneath the skin. The B-mode was used to visualize the location of samples and then the power Doppler mode (gain: 35 dB) was activated. To quantify the vascular volume or blood flow fraction in the scaffold, three slices of PA or Doppler images per mouse (front, middle and rear portion of the scaffold) were acquired. Vascular volume or blood flow signal was evaluated by counting colored pixels in a region of interest (ROI) on a slice using the magic tool in Photoshop CS6, and the value was estimated as the ratio of the number of colored pixels to the total number of pixels in the ROI [38].

2.9. Histology and immunohistochemistry assay

At the designated time points, the mice were euthanized and the four types of implants were removed and immediately fixed in buffered formalin (10%) for 24 h. After extensive washes, the specimens of Collagen/Channel/β-TCP and Collagen/HUVEC/β-TCP were decalcified by 50 mM EDTA for 7 days. Then the decalcified samples and collagen-based samples were gradually dehydrated in a series of ethanol solutions, embedded in paraffin, and sectioned into 7 μm thick slices. Hematoxylin and eosin (H&E) staining was performed on 7 μm thick sections for the observation of blood vessels containing erythrocytes. To evaluate whether the capillary-like networks formed in the grafts in vitro developed into functional perfused blood vessels in vivo, immunohistochemistry staining was carried out on sections. The paraffin sections were first de-paraffinized and treated by an antigen retrieval solution at 95–100 °C for 20 min, then the sections were blocked by 5% goat blocking serum for 1 h. A monoclonal primary antibody rabbit anti-human CD31 antibody (Clone EP3095 for human microvessel detection; 1:500; Millipore) was used. Biotinylated goat anti-rabbit secondary antibodies (1:500; Vector Laboratories) and DAB substrate (Vector Laboratories) were added, followed by hematoxylin counterstaining and permanent mounting. To quantify the density of blood vessels formed in the grafts and the lumens anastomosed with host vasculature, eight randomly selected stained sections from the experimental mice were used (under 40× magnification). The blood vessels were identified as luminal structures containing red blood cells. The functional perfused blood vessels were identified as intact human lumens, which contain murine erythrocytes. To further observe the anastomosis between preformed human capillary networks with host vascular, double immunofluorescence staining on paraffin sections was used to observe the expressions of human CD31 and mouse CD31. Anti-human primary CD31 antibody (Clone EP3095 for human microvessel detection; 1:500; Millipore) and Alexa Fluor® 647 anti-mouse CD31 (1:500, Invitrogen, USA) were used. The procedure of double staining is the same as the procedure of immunofluorescent staining.

2.10. Statistical analysis

The values reported for the density of whole blood vessels and anastomosed functional blood vessels are the mean values ± the standard deviation. Significant difference was statistically analyzed by two-way analysis of variance (ANOVA) and considered if the P value was less than 0.05.

3. Results

3.1. Network formation

An endothelium-lined microchannel in the collagen-based or collagen-β-TCP-based synthetic graft was produced by the CED technique (Fig. 1b and c and Fig. S.1). Before assembly, HUVECs were first cultured on an oligopeptide-coated rod and allowed to reach confluence and to form a dense, uniform cell monolayer (Fig. 1d(i)). During assembly, the endothelial layer was electrochemically detached from the rod onto the surrounding collagen, and an intact endothelium-lined microchannel was created in the collagen (Fig. 1d(ii and iii)). The HUVECs subsequently migrated into the surrounding collagen of the graft from the microchannel (Fig. 1d(iv)). These results indicate that a CED-engineered endothelium in the collagen or channeled macroporous β-TCP scaffold was a network-sprouting source for further vascularization of the entire graft.

To further study the formation of microvascular networks in the collagen-based grafts, we performed immunofluorescent staining of the platelet endothelial cell adhesion molecule (PECAM-1 or CD31). The fluorescent images reveal extensive sprouting branches from the endothelium-lined microchannel and the formation of networks across the collagen-based grafts (Fig. 2). A 3-D reconstituted confocal image demonstrates the formation of 3-D capillary-like networks in the entire area after 7 days' incubation (Fig. 2a). Fig. 2b shows a longitudinal view of a sprouting microchannel under a perfusion condition after 7 days' incubation. At a higher magnification (Fig. 2b(i)), we observed that HUVECs formed many networks from the endothelium-lined microchannel. Furthermore, the immunofluorescent staining of CD31 on paraffin sections clearly shows a few sprouting branches of HUVECs from an endothelium-lined microchannel into the surrounding collagen (Fig. 2c).

3.2. Functional blood flow and vascular network formation in vivo

To evaluate whether the prevascularized collagen-based and collagen-β-TCP-based grafts can promote the functional vascularization, we implanted four types of grafts into immunodeficient mice, including Collagen/HUVEC, Collagen/Channel, Collagen/HUVEC/β-TCP and Collagen/Channel/β-TCP. We used PA imaging and high-frequency power Doppler ultrasound imaging to observe the formation of blood vessels and blood flow in the scaffolds. Due to a lack of ultrasound energy absorption in collagen under the ultrasound system, the systems cannot detect the two groups of

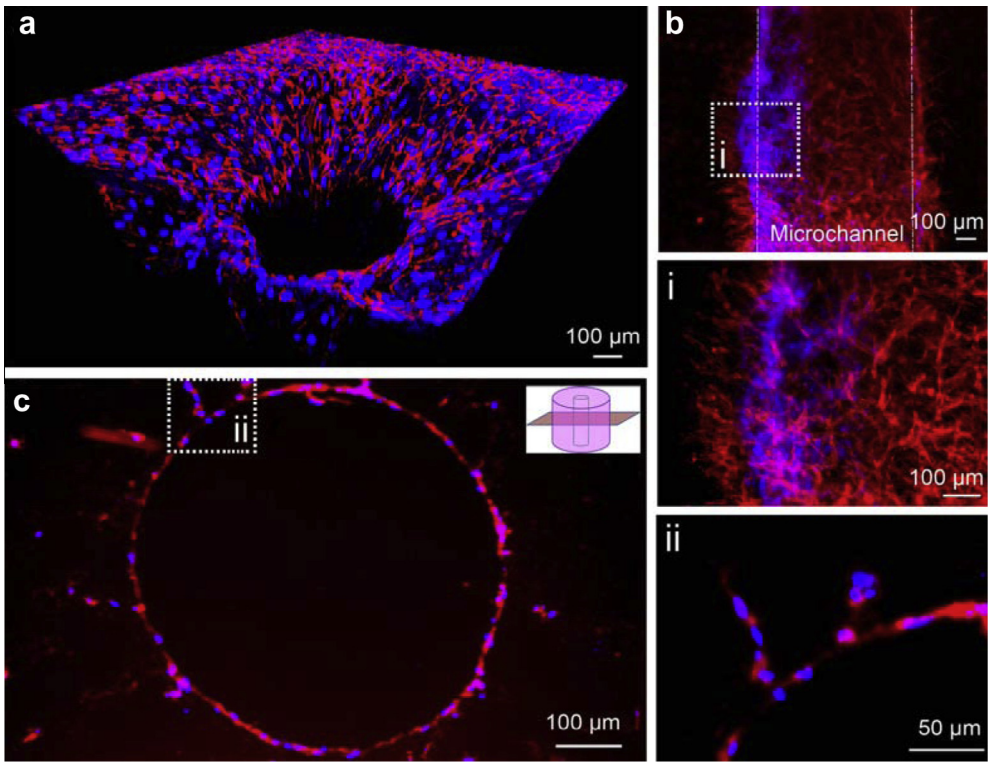

Fig. 2. Immunofluorescent images of human CD31 show network formation. (a) A reconstituted 3-D confocal image shows the microcapillary networks extending to peripheral collagen matrix in a radial way. (b) A longitudinal view of a sprouting microchannel under a perfusion condition after 7 days' incubation and these networks at a high magnification (i). (c) An immunofluorescent staining of CD31 on a paraffin section shows the capillary sprouting of HUVECs from the microchannel at a cross-section view, and two sprouting branches at a higher magnification (ii) (red: CD31; blue: nuclei).

collagen-only grafts (Collagen/Channel and Collagen/HUVEC). For the ceramic-based groups (Collagen/Channel/β-TCP and Collagen/HUVEC/β-TCP), PA images in Fig. 3a indicate that blood vessels presented in the Collagen/HUVEC/β-TCP scaffold between skin and muscle layer by day 7 (ii), and significantly more blood vessels presented across the entire graft by day 14 (iv). A similar trend, but with relatively fewer blood vessels, was observed in the Collagen/Channel/β-TCP graft (Fig. 3a(i, iii)). Quantitative results show that there is a significant difference in vascular volume formed in the two groups ($P < 0.05$). The vascular volume in the Collagen/HUVEC/β-TCP group is significantly higher than that in the Collagen/Channel/β-TCP group (Fig. 3c(ii)). Doppler images in Fig. 3b show that there was blood flow in the two groups and the area of blood flow increased with time. At day 7, the blood flow was first observed in the central microchannel of the graft, and at day 14 the blood flow spread to the surrounding area of the graft. Doppler videos (Videos S1 and S2) show the real-time blood flow in the grafts. Quantitative results show that the signal intensities of the blood flow in the two groups at the two investigated times are significantly different (Fig. 3c(iii)). In the Collagen/HUVEC/β-TCP group, the density of blood flow at days 7 (Fig. 3b(ii)) and 14 (Fig. 3b(iv)) was higher than those in the Collagen/Channel/β-TCP group (Fig. 3b(i, iii)). This result indicates that the endothelium-lined microchannel in the Collagen/HUVEC/β-TCP group promoted blood flow compared to the Collagen/Channel/β-TCP group.

At the designated implantation time, we harvested the four types of implanted grafts (Fig. 4a(i)). Macroscopic views show the gross shapes of the implanted grafts on the subcutaneous tissue after 14 days (Fig. 4a(ii–v)). We see that the collagen-based grafts were compressed into thin slices (Fig. 4a(ii, v)). They lost height after implantation, significant deformation occurred and microchannels were not maintained (Fig. 4a(ii, v)). In the β-TCP-based grafts, host vasculature invaded into the grafts (Fig. 4a(iii, iv)). The rigid β-TCP scaffolds maintained the overall shape and size of the collagen-β-TCP-based grafts and prevented their deformation from the contraction of skin and muscles.

H&E staining indicates that the blood vessels formed in the grafts. At day 7, sparse murine cells invaded the edge zones in the Collagen/Channel samples (Fig. 4b(i)). Compared to the Collagen/Channel samples, the Collagen/HUVEC group had many cells in the collagen (Fig. 4b(ii)). With increasing time, murine cells did not significantly increase in the Collagen/Channel group, and only a few murine cells were still observed in the superficial zone at day 14 (Fig. 4b(v)). However, more cells grew into the Collagen/HUVEC group and some vessels were observed in the surface zone of the gel at day 14 (Fig. 4b(vi)). For the Collagen/Channel/β-TCP grafts, a few murine cells grew into the pores of the peripheral β-TCP zone at day 7 (Fig. 4b(iii)) and a few vessels formed in the graft at day 14 (Fig. 4b(vii)). In contrast, in the Collagen/HUVEC/β-TCP group, not only did many cells grow into the pores of the β-TCP zone, but also blood vessels grew in the graft (Fig. 4b(iv, viii)). These images show that cells and blood vessels more rapidly invaded into Collagen/HUVEC/β-TCP grafts than the other grafts. Quantitative results reveal that the density of blood vessels in the Collagen/HUVEC/β-TCP group is significantly higher than that in the other groups at day 7 and day 14 (Fig. 4c). It is worth noting that the microchannel in the collagen-β-TCP-based grafts was infiltrated with tissue, which made it difficult to observe the boundary of the microchannel.

3.3. Effective vascular anastomosis in vivo

We further performed immunohistochemical staining on anti-human CD31 (hCD31) to investigate whether the in vitro pre-formed HUVEC-derived networks in the grafts can anastomose with the host vasculature. The anastomosis is defined as intact

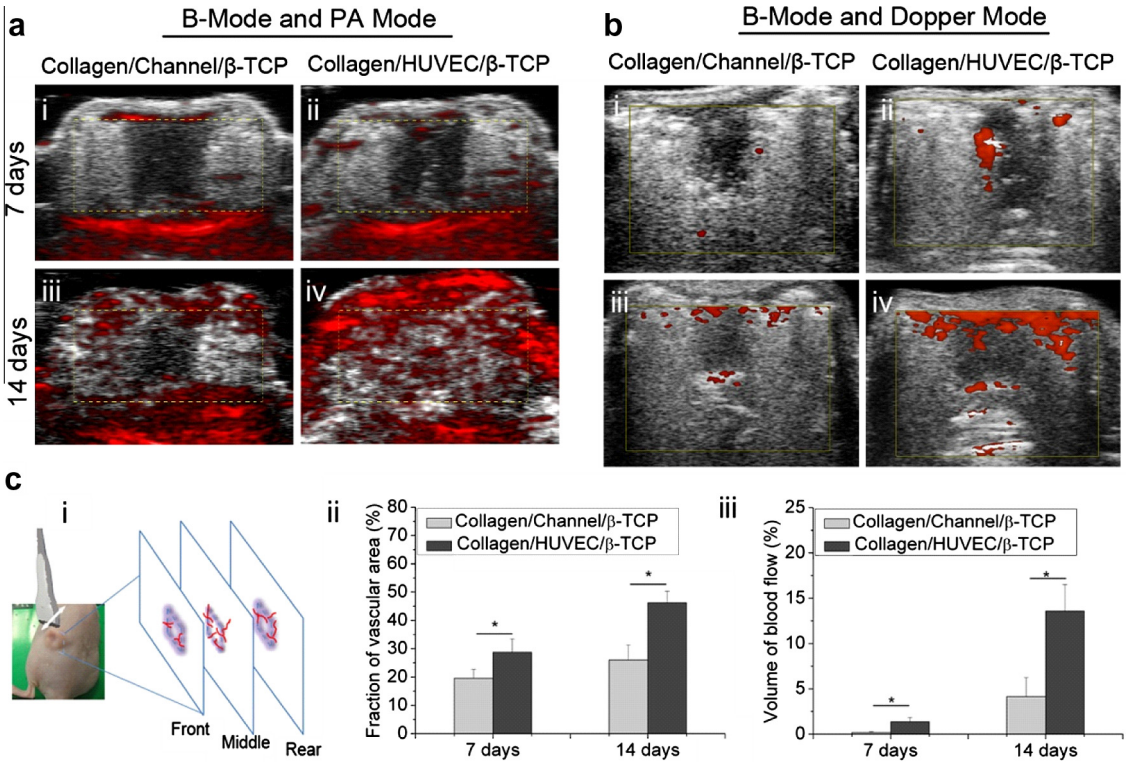

Fig. 3. Evaluations of the vascular volume and the blood flow in scaffolds from PA imaging and high-frequency Doppler ultrasound imaging systems. (a) B-mode and PA mode indicate the vascular volume in Collagen/Channel/β-TCP (i, iii) and Collagen/HUVEC/β-TCP (ii, iv) grafts at days 7 and 14 (yellow dotted box indicates the location of scaffold). (b) B-mode and Doppler mode indicate the blood flow density in Collagen/Channel/β-TCP (i, iii) and Collagen/HUVEC/β-TCP(ii, iv) at days 7 and 14 (yellow box indicates the location of scaffold). (c) Quantification of the vascular volume and blood flow density from PA and power Doppler images on days 7 and 14. (i) Transducer probe was moved above the sample and three slices per sample were acquired for quantification. Color pixel density was used to express the vascular volume (ii) and perfused vascular density (blood flow) (iii) in the two groups ($^*P < 0.05$, $n = 4$).

hCD31 expressing lumens containing murine erythrocytes. Results show that few anastomosed blood vessels are seen in the Collagen/HUVEC grafts at days 7 and 14 (Fig. 5a(ii, vi)), but many anastomosed blood vessels are observed in the Collagen/HUVEC/β-TCP grafts (Fig. 5a(iv, viii)). Quantitative results show that the density of the positive stained hCD31vessels in the Collagen/HUVEC/β-TCP implants (44 ± 11 vessels mm^{-2}) is significantly higher than that in the Collagen/HUVEC implants (23 ± 8 vessels mm^{-2}) at day 14 (Fig. 5b). Furthermore, the densities in the Collagen/HUVEC and Collagen/HUVEC/β-TCP grafts at day 14 are significantly higher than those at day 7, respectively.

Double immunofluorescence staining of anti-human CD31 and anti-mouse CD31 expressions further showed the anastomosed overlap sites between the preformed HUVEC-derived capillaries and the host vasculature (Fig. 5c and Fig. S.3). At day 14, in the Collagen/Channel and Collagen/Channel/β-TCP grafts without HVUECs, only anti-mouse CD31 expression was observed (Fig. 5c(i, iii)), but in the Collagen/HUVEC and Collagen/HUVEC/β-TCP samples, expression of anti-human CD31 (green) and anti-mouse CD31 (magenta) was strongly observed along with some overlap points (yellow) (Fig. 5c(ii, iv)). Furthermore, overlapping intact lumens were also observed in the Collagen/HUVEC/β-TCP samples (Fig. 5c(iv), white arrow). These results suggest that the in vitro preformed human-derived networks successfully anastomosed with the host vasculature.

4. Discussion

In this study we implemented a CED technique to produce an endothelium-lined microchannel and used it to prevascularize a channeled macroporous ceramic scaffold. Results showed that the interconnected macropores of the ceramic scaffold facilitated easy infiltration and homogenous distribution of collagen across the rigid scaffold. The endothelial cell layer on the rod was rapidly transferred onto the collagen and formed an endothelium-lined microchannel after removal of the rod. The presence of the integral endothelium on the microchannel significantly promoted the network formation in vitro and vascularization of the grafts in vivo.

We found that extensive blood flow and anastomosis were generated in the Collagen/HUVEC/β-TCP grafts (Figs. 3–5). In contrast, in the microchannel-containing collagen-based grafts, few cells grew into the collagen-based grafts and cells appeared only in the superficial border regions and few capillary vessels invaded or formed (Fig. 4b(i, ii, v, vi)). This result was consistent with previous studies [19,39] in which murine cells mainly infiltrated into collagen borders though natural collagen hydrogels have been extensively applied in the biomedical field due to their outstanding biocompatibility [40,41]. This may possibly result from the following reasons: first, collagen has a relatively low mechanical strength. Upon implantation, contraction of skin and muscles may deform the mechanically weak collagen [42]. Second, osmotic pressure after in vivo implantation may extract water from the collagen, further leading to its contraction, which is likely to flatten the 3-D porous lattice hydrogel network structure [43,44]. Third, the relatively rapid degradation of collagen may cause unstable interface between collagen and surrounding tissue. These factors may cause the collagen to become denser, which probably inhibited cell invasion and vessel formation. However, in the collagen-β-TCP-based grafts, the rigid ceramic structure maintained the 3-D structure and the lattice framework of the collagen inside the scaffold, which facilitates many cells to grow into the structurally stable collagen-β-TCP-based grafts and

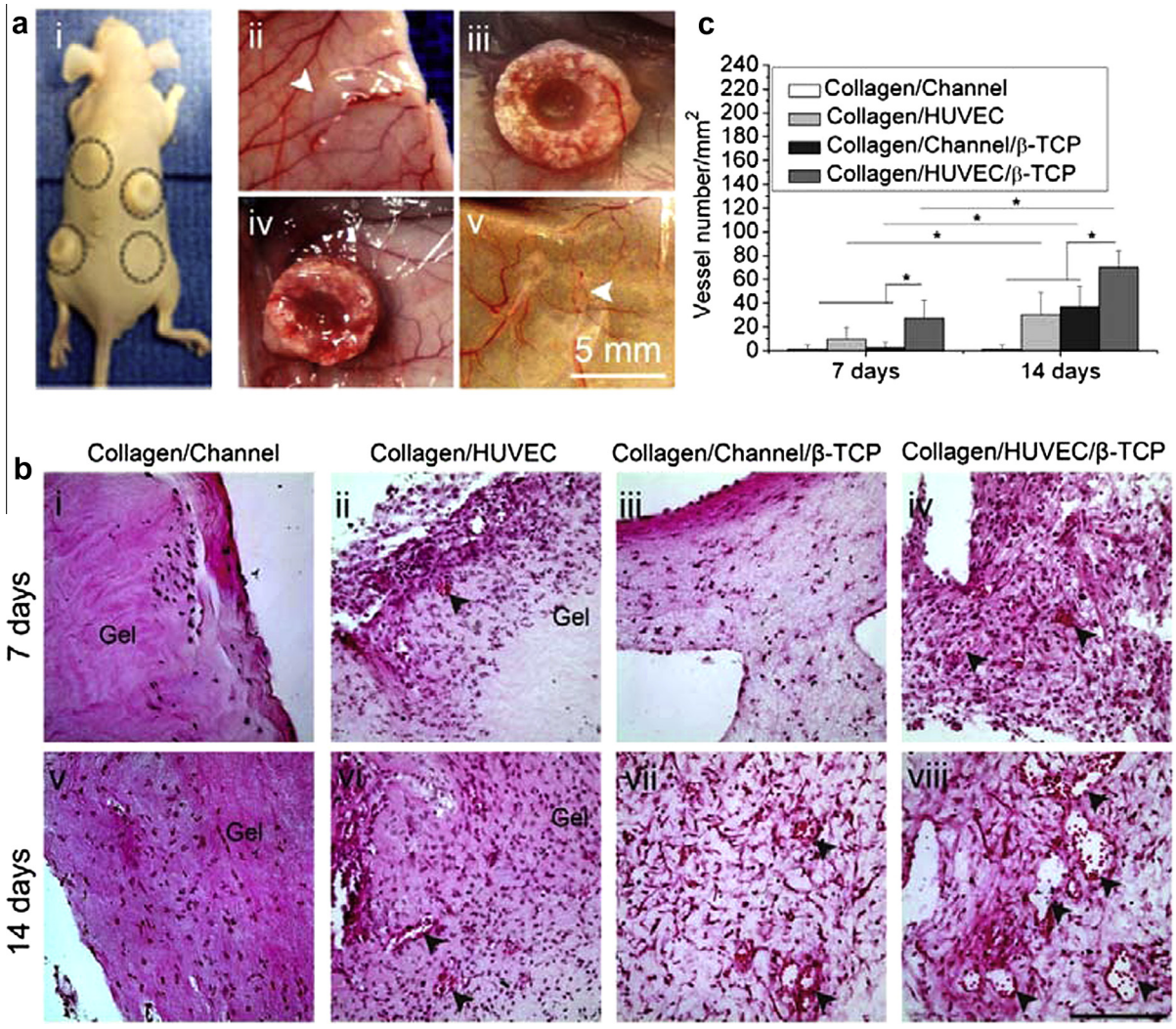

Fig. 4. Histological evaluation of angiogenesis of collagen-based and collagen-β-TCP-based grafts in vivo. (a) Macroscopic views of implants in the back of nude mice (i) and the four types of implants: Collagen/HUVEC (ii), Collagen/HUVEC/β-TCP (iii), Collagen/Channel/β-TCP (iv) and Collagen/Channel (v) on the skin at 14 days after implantation. White arrows show the collagen gels. (b) Representative images of H&E-stained sections from collagen-based and collagen-β-TCP-based grafts at days 7 and 14 (i–viii). Black arrowheads reveal the presence of blood vessels containing murine erythrocytes (scale bar = 100 μm). (c) Vessel density in the constructs over time. The number of vascular-like lumens was quantified for microvessel density ($^*P < 0.05$, $n = 8$).

promote blood vessel development. These results further showed the importance of the integration of soft hydrogel with mechanically sound porous scaffolds for vascularization and tissue engraftment.

Furthermore, it is worth noting that blood flow first occurred in the microchannel of the graft regardless of the presence of endothelial cells, while the presence of endothelial cells demonstrated significantly greater blood flow. This result indicates the critical roles of endothelial cells and microchannels in the vascularization of hydrogel-ceramic-based grafts. Many efforts have been implemented to understand how blood vessels are induced to avascular tissue or grafts [45–47]. Besides endothelial cells and angiogenic signals, microchannels in a tissue-engineered graft have also shown angiogenesis promoting effects compared to a graft in absence of microchannel [48–50]. These results are consistent with our observation that the CED endothelialized microchannel enhanced sprouting and anastomosis. Interestingly, our result also indicated that there was no significant difference in angiogenesis between endothelium-lined collagen grafts (Collagen/HUVEC) and non-endothelialized channels containing collagen/β-TCP grafts (Collagen/Channel/β-TCP). However, it remains unknown in a comparison of angiogenic effects between the microchannel containing hydrogel/β-TCP grafts in the absence of endothelial cells and the endothelial cell encapsulated hydrogel/β-TCP grafts in the absence of microchannels. We also note that this study is limited by the use of HUVEC as a model system on long-term engrafting applications. HUVECs is a well established model system for angiogenesis and vascularization [51,52], but long-term cultures in vitro could also make HUVECs more heterogeneous and have less tube formation capability with in vivo aging [53,54]. In addition, the angiogenic potential of HUVECs isolated from mature macrovasculature has been reported to be weaker than that of human microvasculature endothelial cells [55].

Encouraged by the present results in this study, in the future we will be interested in the vascularization effect of the structural cue such as microchannel containing scaffolds without endothelial cells or the biological cue such as endothelial cell encapsulated scaffolds without microchannels. Furthermore, we will study if and how well the absence or the presence of mesenchymal stem cells, pericytes or smooth muscle cells affect the

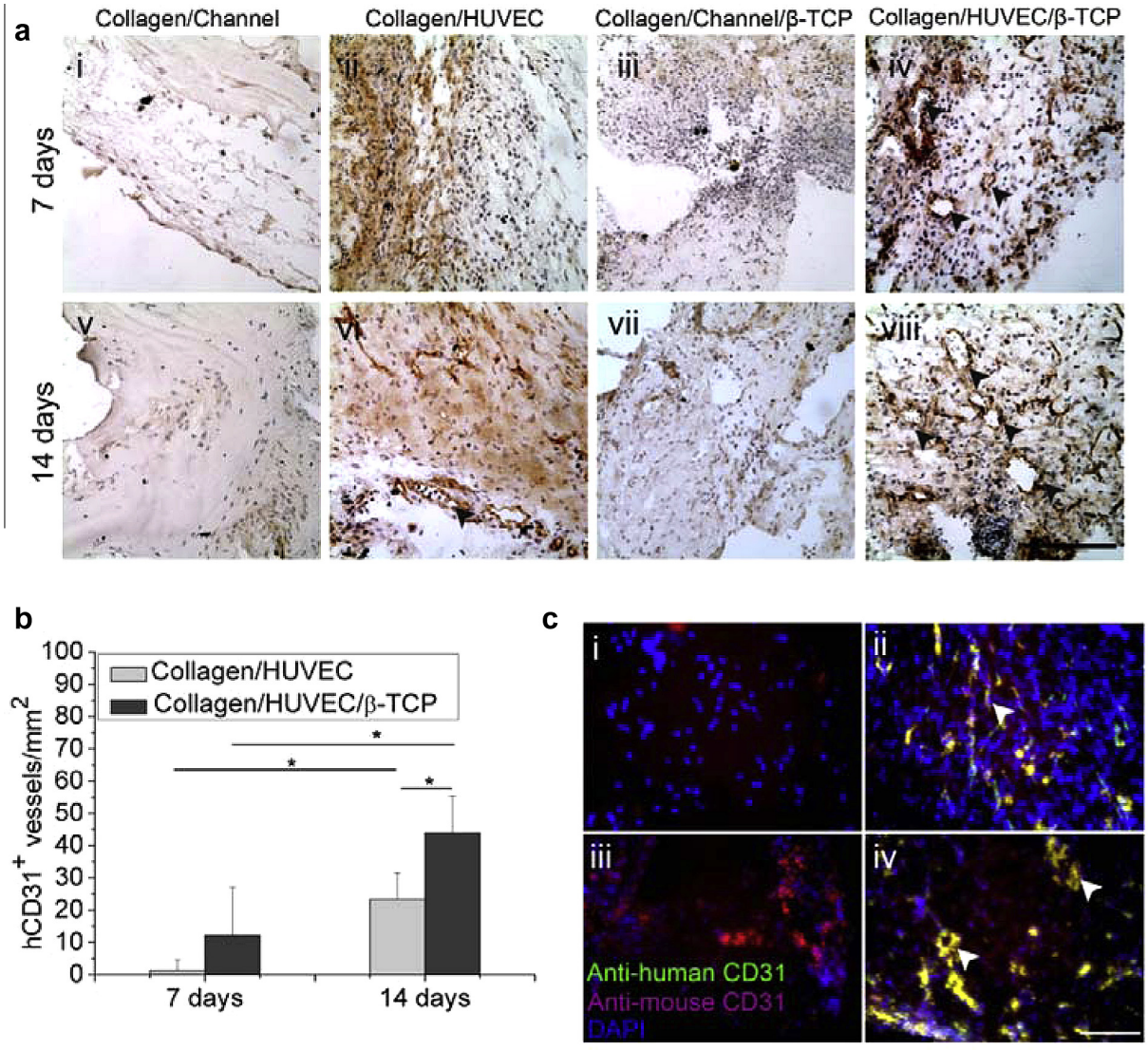

Fig. 5. Immunohistochemistry evaluation of angiogenesis and anastomosis in vivo. (a) Representative immunohistochemistry images of human-CD31 (hCD31) from Collagen/HUVEC and Collagen/HUVEC/β-TCP grafts at days 7 and 14 (i–viii) showed that the hCD31 positive microvessels contain murine erythrocytes (iv, viii) (black arrowheads) (scale bar = 100 μm). (b) The hCD31-positive expressing lumens containing murine erythrocytes were quantified by measuring their density ($^*P < 0.05$, $n = 8$). (c) Immunofluorescent staining of human CD31 (green) and mouse CD31 (magenta) shows the anastomosed sites of preformed human capillaries with host vasculature (white arrows, yellow color). Four groups at day 14 are shown: (i) Collagen/Channel, (ii) Collagen/HUVEC, (iii) Collagen/Channel/β-TCP and (iv) Collagen/HUVEC/β-TCP.

stability of the formed networks, and if and how well a prevascularized network can develop into a mature and stable vasculature and support other cells loaded in the hydrogel-ceramic-based grafts.

The current results from this CED system also motivate further studies about the potential to integrate multiple CED-engineered endothelia with a multi-channeled scaffold as a platform for engineering large tissues regardless of scaffold size. To fully take advantages of this unique electrochemical approach, however, the following limitations should be considered, in particular for multiple channels. First, the quality of the gold coating on a solid rod is essential in support of peptide incorporation, homogenous cell attachment and detachment of intact endothelium. Second, an automatic assembly system will be needed for precise alignment between the multiple endothelium-lined rods and channels of scaffolds. Thus, through improving these limitations, this strategy could provide a flexible platform to engineer large grafts, assemble blood vessel arrays and investigate multicellular organization for broad clinical applications.

5. Conclusion

Here we demonstrated an electrochemical approach to efficiently prevascularize a synthetic collagen–ceramic scaffold. This approach achieves a one-step integration of an intact endothelium and a channeled bioceramic scaffold to promote the functional vascularization of the entire graft. This study also demonstrates the important functional roles of the rigid porous bioceramic scaffold that supports the structural integrity of hydrogel-based microvasculature so it can function in vivo.

Acknowledgements

This work was supported by grants from the following agencies: NIH R01AR057837 (NIAMS), NIH R01DE021468 (NIDCR), DOD W81XWH-10-1-0966 (PRORP), W81XWH-10-200-10 (Airlift Research Foundation), Wallace H. Coulter Foundation, United States, and 11B09003d (NEDO) and 25289291 (MEXT), Japan. We thank Drs Liling Ren and Christopher Browne for the animal

surgery assistance and Dr Liangzhong Xiang for the PA imaging assistance.

Appendix A. Figures with essential colour discrimination

Certain figures in this article, particularly Figs. 1–5 are difficult to interpret in black and white. The full colour images can be found in the on-line version, at http://dx.doi.org/10.1016/j.actbio.2014.09.035.

Appendix B. Supplementary data

Supplementary data associated with this article can be found, in the online version, at http://dx.doi.org/10.1016/j.actbio.2014.09.035.

References

[1] Schek RM, Wilke EN, Hollister SJ, Krebsbach PH. Combined use of designed scaffolds and adenoviral gene therapy for skeletal tissue engineering. Biomaterials 2006;27:1160–6.
[2] Jarcho M. Calcium phosphate ceramics as hard tissue prosthetics. Clin Orthop Relat Res 1981:259–78.
[3] LeGeros RZ. Properties of osteoconductive biomaterials: calcium phosphates. Clin Orthop Relat Res 2002:81–98.
[4] Cuchiara MP, Gould DJ, McHale MK, Dickinson ME, West JL. Integration of self-assembled microvascular networks with microfabricated PEG-based hydrogels. Adv Funct Mater 2012;22:4511–8.
[5] Chen YC, Lin RZ, Qi H, Yang Y, Bae H, Melero-Martin JM, et al. Functional human vascular network generated in photocrosslinkable gelatin methacrylate hydrogels. Adv Funct Mater 2012;22:2027–39.
[6] Eweida AM, Nabawi AS, Abouarab M, Kayed M, Elhammady H, Etaby A, et al. Enhancing mandibular bone regeneration and perfusion via axial vascularization of scaffolds. Clin Oral Investig 2014;18:1671–8.
[7] Beier JP, Horch RE, Hess A, Arkudas A, Heinrich J, Loew J, et al. Axial vascularization of a large volume calcium phosphate ceramic bone substitute in the sheep AV loop model. J Tissue Eng Regen Med 2010;4:216–23.
[8] Epstein SE, Kornowski R, Fuchs S, Dvorak HF. Angiogenesis therapy: amidst the hype, the neglected potential for serious side effects. Circulation 2001;104:115–9.
[9] Novosel EC, Kleinhans C, Kluger PJ. Vascularization is the key challenge in tissue engineering. Adv Drug Deliv Rev 2011;63:300–11.
[10] Wernike E, Montjovent MO, Liu Y, Wismeijer D, Hunziker EB, Siebenrock KA, et al. VEGF incorporated into calcium phosphate ceramics promotes vascularisation and bone formation in vivo. Eur Cell Mater 2010;19:30–40.
[11] Zhou J, Lin H, Fang T, Li X, Dai W, Uemura T, et al. The repair of large segmental bone defects in the rabbit with vascularized tissue engineered bone. Biomaterials 2010;31:1171–9.
[12] Unger RE, Ghanaati S, Orth C, Sartoris A, Barbeck M, Halstenberg S, et al. The rapid anastomosis between prevascularized networks on silk fibroin scaffolds generated in vitro with cocultures of human microvascular endothelial and osteoblast cells and the host vasculature. Biomaterials 2010;31:6959–67.
[13] Wang L, Fan H, Zhang Z-Y, Lou A-J, Pei G-X, Jiang S, et al. Osteogenesis and angiogenesis of tissue-engineered bone constructed by prevascularized β-tricalcium phosphate scaffold and mesenchymal stem cells. Biomaterials 2010;31:9452–61.
[14] Kokemueller H, Spalthoff S, Nolff M, Tavassol F, Essig H, Stuehmer C, et al. Prefabrication of vascularized bioartificial bone grafts in vivo for segmental mandibular reconstruction: experimental pilot study in sheep and first clinical application. Int J Oral Maxillofac Surg 2010;39:379–87.
[15] Unger RE, Sartoris A, Peters K, Motta A, Migliaresi C, Kunkel M, et al. Tissue-like self-assembly in cocultures of endothelial cells and osteoblasts and the formation of microcapillary-like structures on three-dimensional porous biomaterials. Biomaterials 2007;28:3965–76.
[16] Grellier M, Bordenave L, Amedee J. Cell-to-cell communication between osteogenic and endothelial lineages: implications for tissue engineering. Trends Biotechnol 2009;27:562–71.
[17] McGuigan AP, Sefton MV. Vascularized organoid engineered by modular assembly enables blood perfusion. Proc Natl Acad Sci USA 2006;103:11461–6.
[18] Chiu LL, Montgomery M, Liang Y, Liu H, Radisic M. Perfusable branching microvessel bed for vascularization of engineered tissues. Proc Natl Acad Sci USA 2012;109:E3414–23.
[19] Nillesen ST, Geutjes PJ, Wismans R, Schalkwijk J, Daamen WF, van Kuppevelt TH. Increased angiogenesis and blood vessel maturation in acellular collagen-heparin scaffolds containing both FGF2 and VEGF. Biomaterials 2007;28:1123–31.
[20] Golden AP, Tien J. Fabrication of microfluidic hydrogels using molded gelatin as a sacrificial element. Lab Chip 2007;7:720–5.
[21] Ling Y, Rubin J, Deng Y, Huang C, Demirci U, Karp JM, et al. A cell-laden microfluidic hydrogel. Lab Chip 2007;7:756–62.
[22] Choi NW, Cabodi M, Held B, Gleghorn JP, Bonassar LJ, Stroock AD. Microfluidic scaffolds for tissue engineering. Nat Mater 2007;6:908–15.
[23] Cuchiara MP, Allen AC, Chen TM, Miller JS, West JL. Multilayer microfluidic PEGDA hydrogels. Biomaterials 2010;31:5491–7.
[24] Therriault D, White SR, Lewis JA. Chaotic mixing in three-dimensional microvascular networks fabricated by direct-write assembly. Nat Mater 2003;2:265–71.
[25] Wu W, Hansen CJ, Aragon AM, Geubelle PH, White SR, Lewis JA. Direct-write assembly of biomimetic microvascular networks for efficient fluid transport. Soft Matter 2010;6:739–42.
[26] Miller JS, Stevens KR, Yang MT, Baker BM, Nguyen D-HT, Cohen DM, et al. Rapid casting of patterned vascular networks for perfusable engineered three-dimensional tissues. Nat Mater 2012;11:768–74.
[27] Visconti RP, Kasyanov V, Gentile C, Zhang J, Markwald RR, Mironov V. Towards organ printing: engineering an intra-organ branched vascular tree. Expert Opin Biol Ther 2010;10:409–20.
[28] Zorlutuna P, Annabi N, Camci-Unal G, Nikkhah M, Cha JM, Nichol JW, et al. Microfabricated biomaterials for engineering 3D tissues. Adv Mater 2012;24:1782–804.
[29] Nikkhah M, Eshak N, Zorlutuna P, Annabi N, Castello M, Kim K, et al. Directed endothelial cell morphogenesis in micropatterned gelatin methacrylate hydrogels. Biomaterials 2012;33:9009–18.
[30] Zheng Y, Chen J, Craven M, Choi NW, Totorica S, Diaz-Santana A, et al. In vitro microvessels for the study of angiogenesis and thrombosis. Proc Natl Acad Sci USA 2012;109:9342–7.
[31] Sadr N, Zhu M, Osaki T, Kakegawa T, Yang Y, Moretti M, et al. SAM-based cell transfer to photopatterned hydrogels for microengineering vascular-like structures. Biomaterials 2011;32:7479–90.
[32] Mochizuki N, Kakegawa T, Osaki T, Sadr N, Kachouie NN, Suzuki H, et al. Tissue engineering based on electrochemical desorption of an RGD-containing oligopeptide. J Tissue Eng Regen Med 2013;7:236–43.
[33] Seto Y, Inaba R, Okuyama T, Sassa F, Suzuki H, Fukuda J. Engineering of capillary-like structures in tissue constructs by electrochemical detachment of cells. Biomaterials 2010;31:2209–15.
[34] Osaki T, Kakegawa T, Suzuki H, Fukuda J. Electrical detachment of cells for engineering capillary-like structures in a photocrosslinkable hydrogel. Conf Proc IEEE Eng Med Biol Soc 2011;2011:2451–4.
[35] Liu Y, Kim JH, Young D, Kim S, Nishimoto SK, Yang Y. Novel template-casting technique for fabricating beta-tricalcium phosphate scaffolds with high interconnectivity and mechanical strength and in vitro cell responses. J Biomed Mater Res A 2010;92:997–1006.
[36] Kang Y, Kim S, Khademhosseini A, Yang Y. Creation of bony microenvironment with CaP and cell-derived ECM to enhance human bone-marrow MSC behavior and delivery of BMP-2. Biomaterials 2011;32:6119–30.
[37] Kang Y, Scully A, Young DA, Kim S, Tsao H, Sen M, et al. Enhanced mechanical performance and biological evaluation of a PLGA coated beta-TCP composite scaffold for load-bearing applications. Eur Polym J 2011;47:1569–77.
[38] Chen JJ, Fu SY, Chiang CS, Hong JH, Yeh CK. A preclinical study to explore vasculature differences between primary and recurrent tumors using ultrasound Doppler imaging. Ultrasound Med Biol 2013;39:860–9.
[39] Chen Y-C, Lin R-Z, Qi H, Yang Y, Bae H, Melero-Martin JM, et al. Functional human vascular network generated in photocrosslinkable gelatin methacrylate hydrogels. Adv Funct Mater 2012;22:2027–39.
[40] Meena C, Mengi SA, Deshpande SG. Biomedical and industrial applications of collagen. Proc Indian Acad Sci (Chem Sci) 1999;111:319–29.
[41] Ferreira AM, Gentile P, Chiono V, Ciardelli G. Collagen for bone tissue regeneration. Acta Biomater 2012;8:3191–200.
[42] Vernon RB, Sage EH. Contraction of fibrillar type I collagen by endothelial cells: a study in vitro. J Cell Biochem 1996;60:185–97.
[43] Bell E, Ivarsson B, Merrill C. Production of a tissue-like structure by contraction of collagen lattices by human fibroblasts of different proliferative potential in vitro. Proc Natl Acad Sci USA 1979;76:1274–8.
[44] Kolodney MS, Wysolmerski RB. Isometric contraction by fibroblasts and endothelial cells in tissue culture: a quantitative study. J Cell Biol 1992;117:73–82.
[45] Djonov V, Schmid M, Tschanz SA, Burri PH. Intussusceptive angiogenesis: its role in embryonic vascular network formation. Circ Res 2000;86:286–92.
[46] Iruela-Arispe ML, Davis GE. Cellular and molecular mechanisms of vascular lumen formation. Dev Cell 2009;16:222–31.
[47] Song JW, Bazou D, Munn LL. Anastomosis of endothelial sprouts forms new vessels in a tissue analogue of angiogenesis. Integr Biol (Camb) 2012;4:857–62.
[48] Gui L, Niklason LE. Vascular tissue engineering: building perfusable vasculature for implantation. Curr Opin Chem Eng 2014;3:68–74.
[49] Bertassoni LE, Cecconi M, Manoharan V, Nikkhah M, Hjortnaes J, Cristino AL, et al. Hydrogel bioprinted microchannel networks for vascularization of tissue engineering constructs. Lab Chip 2014;14:2202–11.
[50] Wang XY, Jin ZH, Gan BW, Lv SW, Xie M, Huang WH. Engineering interconnected 3D vascular networks in hydrogels using molded sodium alginate lattice as the sacrificial template. Lab Chip 2014;14:2709–16.
[51] Boisen L, Drasbek KR, Pedersen AS, Kristensen P. Evaluation of endothelial cell culture as a model system of vascular ageing. Exp Gerontol 2010;45:779–87.
[52] Park HJ, Zhang Y, Georgescu SP, Johnson KL, Kong D, Galper JB. Human umbilical vein endothelial cells and human dermal microvascular endothelial cells offer new insights into the relationship between lipid metabolism and angiogenesis. Stem Cell Rev 2006;2:93–102.

[53] Yang J, Chang E, Cherry AM, Bangs CD, Oei Y, Bodnar A, et al. Human endothelial cell life extension by telomerase expression. J Biol Chem 1999;274:26141–8.
[54] Ha JM, Kim MR, Oh HK, Lee BH, Ahn HY, Shin JC, et al. Outgrowing endothelial progenitor-derived cells display high sensitivity to angiogenesis modulators and delayed senescence. FEBS Lett 2007;581:2663–9.
[55] Jackson CJ, Nguyen M. Human microvascular endothelial cells differ from macrovascular endothelial cells in their expression of matrix metalloproteinases. Int J Biochem Cell Biol 1997;29:1167–77.